SYNTHESIS, STRUCTURAL CHARACTERISATION AND ELECTROCHEMISTRY OF BIS[(DIPHENYLPHOSPHINO)-FERROCENE]DIRUTHENIUM COMPLEXES $[Ru_2(\mu\text{-}RCO_2)_2(CO)_4(FcPPh_2)_2]$ (R = H AND Me)

Petr Štěpnička[1,*] and Ivana Císařová[2]

Department of Inorganic Chemistry, Faculty of Science, Charles University, Hlavova 2030, 128 40 Prague 2, Czech Republic;
e-mail: [1] stepnic@natur.cuni.cz, [2] cisarova@natur.cuni.cz

Received January 28, 2009
Accepted March 15, 2009
Published online April 21, 2009

Dedicated to Alfred Bader on the occasion of his 85th birthday.

Polymeric carboxylatoruthenium complexes $[Ru_2(\mu\text{-}RCO_2)_2(CO)_4]_n$ (**1**, R = H; **2**, R = Me) react with (diphenylphosphino)ferrocene ($FcPPh_2$) to give the corresponding discrete diruthenium complexes $[Ru_2(\mu\text{-}RCO_2)_2(CO)_4(FcPPh_2)_2]$ (**3**, R = H; **4**, R = Me) in good yields. Compounds **3** and **4** were characterised by spectroscopic (NMR, IR and MS) and voltammetric methods. The crystal structure of **4** was determined by single-crystal X-ray diffraction.
Keywords: Ruthenium; Ferrocene ligands; Phosphines; Sawhorse complexes; Electrochemistry; Structure elucidation.

Carboxylate-bridged diruthenium complexes $[Ru_2(\mu\text{-}RCO_2)_2(CO)_4L_2]$, where L is a monodentate ligand, typically a phosphine or nitrogen donor, have attracted considerable attention since their discovery in the late 1960's[1]. In addition to being structurally interesting compounds, these complexes are also of multiple practical use. Prominent fields for their utilisation include applications in various Ru-catalysed organic reactions[2], in the preparation of liquid-crystalline materials[3], and in the design of metal-organic frameworks[4].

We have recently prepared and studied several carboxylate-bridged diruthenium complexes bearing redox-active ferrocenyl groups in the carboxylate and/or in the L subunits[5]. As an extension of our work, this contribution reports the synthesis, structural characterisation and electrochemistry of complexes $[Ru_2(\mu\text{-}RCO_2)_2(CO)_4(FcPPh_2)_2]$ (Fc = ferrocenyl)

doi:10.1135/cccc2009003

derived from simple organic acids (R = H and Me) and redox active (diphenylphosphino)ferrocene.

RESULTS AND DISCUSSION

Synthesis and Characterisation

In analogy with simple (organic) phosphines[1], the reaction between (diphenylphosphino)ferrocene and polymeric carboxylatoruthenium complexes $[Ru_2(\mu\text{-}RCO_2)_2(CO)_4]_n$ (**1**, R = H; **2**, R = Me) in refluxing toluene afforded the respective diruthenium complexes $[Ru_2(\mu\text{-}RCO_2)_2(CO)_4(PPh_2Fc)_2]$ (**3** and **4**; Scheme 1). The complexes were isolated as yellow (**3**) or orange (**4**) air-stable solids in good yields and were characterised by combustion analyses and conventional spectroscopic methods. In addition, the structure of **4** was established by single-crystal X-ray diffraction analysis (vide infra). A similar reaction of **2** with 1′-(diphenylphosphino)ferrocene-1-carboxylic acid (Hdpf)[6] yielded an insoluble material. This product is very likely a coordination polymer in which the corresponding phosphinocarboxylate (dpf^-) coordinates as a phosphine and, simultaneously, replaces the acetate ligand, hence acting as a bridge between distinct diruthenium units.

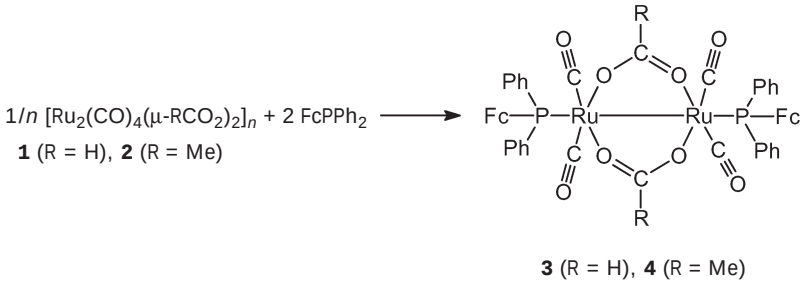

SCHEME 1

Complexes **3** and **4** display abundant molecular ions in soft-ionisation (LSI) mass spectra with characteristic isotopic patterns. Their IR spectra are dominated by strong ν(C≡O) bands in the range 1925–2030 cm^{-1} due to the terminal carbonyl ligands and by the carboxylate bands at 1600 cm^{-1} (**3**) or 1576 cm^{-1} (**4**) (cf. ref.[1]). ^1H and ^{31}P NMR spectra of **3** and **4** are in accordance with the formulation, showing characteristic signals of the carboxylate and phosphine ligands (^1H NMR, RCO_2: δ_H 8.32 ppm for **3**, and 1.85 ppm for **4**; ^{31}P NMR: singlets at $\delta_P \approx +5$ ppm). The ^{13}C NMR signals of

the carbonyl ligands were observed at δ_C ca. 205 ppm (C≡O), and those due to the carboxylate bridges at δ_C 176.1 and 185.7 ppm for **3** and **4**, respectively. The ^{13}C NMR spectra have further corroborated the bis(phosphine) nature of the complexes, displaying the resonances of the phosphinylated aromatic rings (the C and CH groups in the cyclopentadiene and benzene rings except for the phenyl CH_{para} group), the signals of the carboxylate (COO) and carbonyl (C≡O) ligands as virtual triplets that typically arise in ABX spin systems of the type ^{12}C-$^{31}P(A)$-M-$^{31}P(B)$-$^{13}C(X)$ (M = metal)[7,8].

*Crystal Structure of **4***

Compound **4** crystallises in a monoclinic lattice (space group $P2_1/c$), forming a molecular crystal assembly defined by the van der Waals envelope of the complex molecule. A view of the molecular structure is presented in Fig. 1. Selected bond distances and angles are given in Table I.

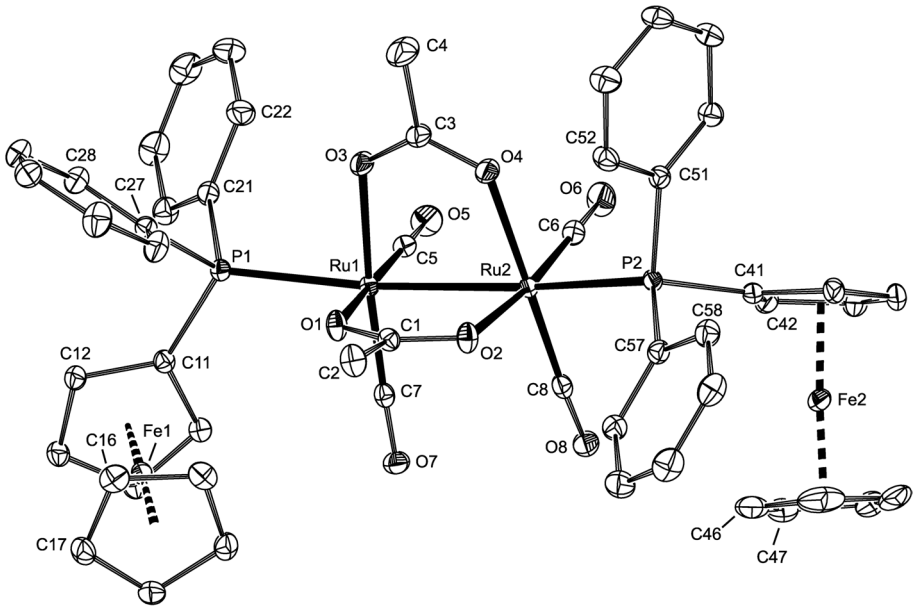

FIG. 1
A view of the molecular structure of complex **4**. Hydrogen atoms were omitted for clarity. Displacement ellipsoids correspond to the 30% probability level

TABLE I
Selected bond distances (in Å) and angles (in °) for **4**[a]

Ru1–Ru2	2.7388(2)	P1–Ru1–Ru2–P2	22.6(2)
Ru1–P1	2.4520(5)	Ru2–P2	2.4180(5)
Ru1–O1	2.128(2)	Ru2–O2	2.126(2)
Ru1–O3	2.127(2)	Ru2–O4	2.123(2)
Ru1–C5	1.838(2)	Ru2–C6	1.850(2)
Ru1–C7	1.848(2)	Ru2–C8	1.852(2)
O1–C1	1.257(3)	O3–C3	1.258(3)
O2–C1	1.256(3)	O4–C3	1.257(3)
C1–C2	1.507(3)	C3–C4	1.508(4)
C5–O5	1.149(3)	C6–O6	1.145(3)
C7–O7	1.151(3)	C8–O8	1.148(3)
P1–Ru1–Ru2	170.43(1)	P2–Ru2–Ru1	166.73(2)
P1/Ru2–Ru1–O1	91.57(4)/82.58(4)	P2/Ru1–Ru2–O2	85.73(4)/83.41(4)
P1/Ru2–Ru1–O3	87.25(4)/84.59(4)	P2/Ru1–Ru2–O4	89.56(4)/81.58(4)
P1/Ru2–Ru1–C5	92.31(7)/93.08(7)	P2/Ru1–Ru2–C6	96.84(7)/93.17(7)
P1/Ru2–Ru1–C7	98.29(6)/89.64(6)	P2/Ru1–Ru2–C8	93.21(7)/96.14(7)
O1–Ru1–O3	83.73(6)	O2–Ru2–O4	83.00(6)
O1–Ru1–C7	93.27(8)	O2–Ru2–C8	99.84(8)
O3–Ru1–C5	92.78(8)	O4–Ru2–C6	90.84(8)
C5–Ru1–C7	89.82(9)	C6–Ru2–C8	86.2(1)
O1–C1–O2	124.9(2)	O3–C3–O4	125.7(2)
Ru1–C5–O5	179.6(2)	Ru2–C6–O6	179.6(2)
Ru1–C7–O7	178.1(2)	Ru2–C8–O8	174.8(2)
Fe1–Cg1	1.644(1)	Fe2–Cg3	1.643(1)
Fe1–Cg2	1.659(1)	Fe2–Cg4	1.656(1)
∠Cp1,Cp2	1.8(1)	∠Cp3,Cp4	4.9(2)

[a] Definition of the ring planes: Cp1 = C(11–15), Cp2 = C(16–20), Cp3 = C(41–45), Cp4 = C(46–50), Cg*n* (*n* = 1–4) denote the respective ring centroids.

The molecule of **4** has a "sawhorse" geometry typical of $[Ru_2(\mu\text{-}RCO_2)_2(CO)_4L_2]$ complexes, where L is a monodentate ligand. The Ru–Ru distance of 2.7388(2) Å falls among those observed in structurally characterised $[Ru_2(\mu\text{-}RCO_2)_2(CO)_4L_2]$ complexes with phosphine ligands[9], being particularly close to the Ru–Ru distances reported for $[Ru_2(\mu\text{-}CH_3CO_2)_2(CO)_4\{P(i\text{-}Pr_3)_2\}]$ (2.738(1) Å, ref.[2l]) and $[Ru_2(\mu\text{-}CH_3CO_2)_2(CO)_4(PPh_3)_2]$ (2.7411(8) Å, ref.[10]). Individual Ru–donor distances are rather unexceptional, comparing favourably with the data reported for the mentioned reference compounds.

The *cis*-arranged carbonyl ligands occupy the positions opposite to the bridging acetate groups, and are slightly bent (Ru–C≡O 174.8(2)–179.6(2)°). Atoms forming the Ru1–O–C–O–Ru2 rings are coplanar within less than ca. 0.08 Å, and the CO_2Ru_2 ring planes subtend a dihedral angle 82.91(5)°. When viewed along the Ru1–Ru2 bond, the $\{RuO_2C_2\}$ moieties are eclipsed. However, the limited O···O distance in the carboxylate bridges (O1···O2 2.228(2), O3···O4 2.238(2) Å) leads to an inclination of their bridged edges. The dihedral angle of the {Ru1,O1,O3,C5,C7} and {Ru2,O2,O4,C6,C8} least-squares planes[11] is 14.26(8)° (Fig. 2).

The peripheral phosphine ligands further lower the overall molecular symmetry. They not only coordinate somewhat asymmetrically (cf. Ru1–P1 2.4520(5) and Ru2–P2 2.4180(5) Å; P1–Ru1–Ru2 170.43(1) and P2–Ru2–Ru1 166.73(2)°) but also assume different orientations with respect to the diruthenium core. The statistically significant difference in the Ru–P bond lengths (0.034 Å) can be accounted for by the different orientations of the ferrocenyl moieties with respect to the central $Ru_2(\mu\text{-}CH_3CO_2)_2(CO)_4$ unit. The shorter Ru2–P2 bond is associated with the phosphine ligand whose

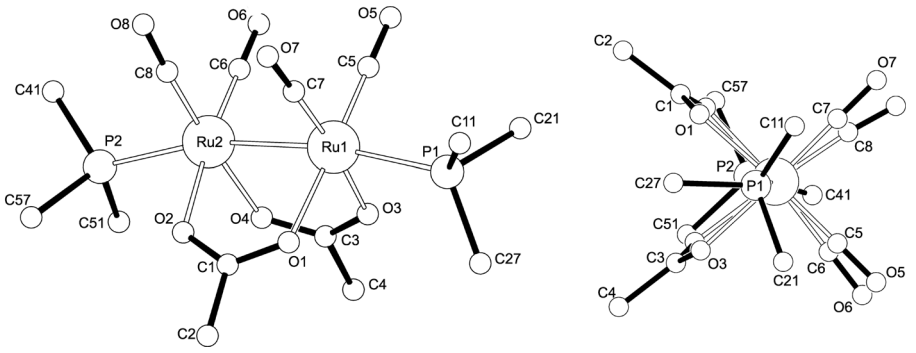

FIG. 2
The dinuclear core in **4**: a general view and b projection along the Ru1–Ru2 vector

ferrocenyl group is located in the wedge defined by the CO ligands whereas the longer Ru1–P1 bond is observed for the phosphine whose ferrocenyl group is directed into the 'quadrant' defined by the CO and acetate ligands which, in combination, are sterically more demanding than two carbonyls. Both ligating phosphorus atoms are displaced from the Ru1–Ru2 axis into the wedge formed by the carboxyl groups (Fig. 2b). The angles subtended by the Ru1–P1/Ru1–Ru2 and Ru2–P2/Ru1–Ru2 vectors are ca. 10 and 13°, respectively, which corresponds to lateral shifts from the Ru1–Ru2 axis by ca. 0.4 and 0.6 Å for P1 and P2 (cf. the P1–Ru1–Ru2 and P2–Ru2–Ru1 angles in Table I). Consequently, the $Ru_2O_4C_4P_2$ complex core is considerably bent along its longest axis and also twisted, showing the P1–Ru1–Ru2–P2 torsion angle as high as 22.6(2)°. A similar value, 21.9(9)°, was reported for $[Ru_2(\mu\text{-}CH_3CO_2)_2(CO)_4\{P(t\text{-}Bu)_3\}_2]$ whilst the $P(i\text{-}Pr)_3$ analogue showed a twist of only 2.5(7)° (ref.[21]). On the other hand, the geometry of the peripheral ferrocene groups is quite regular. The Fe–ring centroid distances are 1.644(1) Å (Fe1) and 1.643(1) Å (Fe2) for the phosphinylated cyclopentadiene rings, and 1.659(1) Å (Fe1) and 1.656(1) Å (Fe2) for the unsubstituted ones. The cyclopentadiene rings are tilted only slightly, the dihedral angles of their least-squares planes being 1.8(1)° (Fe1) and 4.9(2)° (Fe2).

Electrochemistry

Complexes **3** and **4** were studied by cyclic voltammetry (CV) at a platinum disc electrode and by linear-sweep voltammetry (LSV) at a rotating platinum disc electrode in dichloromethane solutions. Pertinent data are given in Table II.

TABLE II
Summary of the electrochemical data[a]

Complex	$E_{pa}(I)$, V	$E^{\circ\prime}(II)$, V
3	0.14	0.34
4	0.11	0.36

[a] Recorded at a Pt disc electrode for 0.5 mM analyte in dichloromethane containing 0.2 M Bu_4NPF_6 as the supporting electrolyte. The potentials are given relative to ferrocene/ferrocenium reference. $E^{\circ\prime}$ is defined as an average of the anodic (E_{pa}) and cathodic (E_{pc}) peak potentials from cyclic voltammetry, i.e., $E^{\circ\prime} = 1/2(E_{pa} + E_{pc})$. For irreversible processes, anodic peak potentials from cyclic voltammograms recorded at 100 mV s^{-1} scan rate are quoted.

The electrochemical responses of **3** (Fig. 3) and **4** are similar, reflecting chemical similarity of the complexes. Both complexes undergo two consecutive two-electron oxidations in the potential window provided by the solvent. The first anodic process (wave *I*) is diffusion-controlled and electrochemically irreversible. No reduction counter-peak is seen in CV voltammograms at scan rates up to 5 V s^{-1}. The anodic peak current increases with the square root of the scan rate ($i_{pa} \propto$ (scan rate)$^{1/2}$). In contrast, the following oxidation (wave *II*) is essentially reversible and diffusion-controlled ($i_{pa} \propto$ (scan rate)$^{1/2}$, $i_{pc}/i_{pa} \approx 1$ at scan rates 50–1000 mV s^{-1}). Notably, the heights of the oxidative waves are equal in the first CV cycle ($i_{pa}(I) = i_{pa}(II)$) whereas, in the second and following scans, the first wave appears considerably diminished in height ($i_{pa}(I) < i_{pa}(II)$). In LSV responses, both anodic processes give rise to standard sigmoidal waves of equal heights.

$^{31}P\{^1H\}$ NMR spectra of the 1:1 and 1:2 (molar ratio) **4**:DDQ mixtures (DDQ = 2,3-dichloro-5,6-dicyano-1,4-benzoquinone)[12] indicated that two electrons are removed to complete the first oxidation. After the chemical oxidation, the signals due to **4** are no longer observed, being replaced with several peaks in the region δ_P 38–40. The cyclic voltammogram recorded on a **4**:DDQ mixture containing excess DDQ (slightly more than two equivalents) displayed a wave due to the unreacted oxidising agent and the unaffected wave *II*. The wave *I* was not observed. Attempts to crystallise the product of chemically oxidised **4** did not afford any defined material.

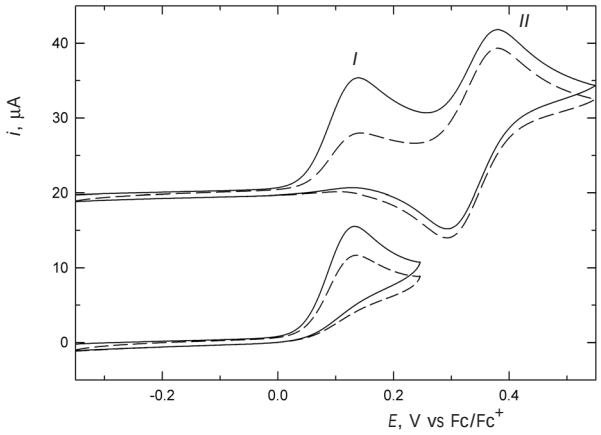

FIG. 3
Cyclic voltammograms of **3** (0.5 mM in dichloromethane, Pt electrode, 100 mV s^{-1} scan rate). For clarity, the second scans are presented with dashed lines and the cyclic voltammograms are onset by 20 μA

Considering the differences in the redox potentials, the wave *I* can be attributed tentatively to an irreversible oxidation of the diruthenium core (formally 1 electron per Ru atom; complex **4** becomes more easily oxidised because of a higher donating ability of acetate bridge). This primary oxidation gives rise to an unstable cation, which undergoes fast chemical change (structural reorganisation) to afford another redox-active species, which becomes oxidised in a single reversible step, probably at the ferrocenyl groups. It should be noted that the redox behaviour of **3** and **4** exhibits some analogy with that of $[Ru_2(\mu\text{-}FcCO_2)_2(CO)_4(PPh_3)_2]$, whereas for $[Ru_2(\mu\text{-}FcCO_2)_2(CO)_4(py)_2]$ (py = pyridine) the waves were observed in the reversed order[5b].

EXPERIMENTAL

Materials and Methods

The syntheses were carried out under an argon atmosphere. Compounds $[Ru_2(\mu\text{-}RCO_2)_2(CO)_4]_n$ (**1**, R = H; **2**, R = CH_3)[1], $FcPPh_2$ (ref.[13]), and Hdpf (ref.[6a]) were prepared by the literature procedures. Toluene was dried over sodium and distilled under argon.

^1H, $^{31}P\{^1H\}$, and $^{13}C\{^1H\}$ NMR spectra were measured at 298 K on a Varian Unity Inova 400 spectrometer. Chemical shifts (δ) are given in ppm relative to internal $SiMe_4$ (^1H, ^{13}C) or external 85% H_3PO_4 (^{31}P). Coupling constants (*J*) are given in Hz. IR spectra were recorded with an FT IR Mattson Genesis spectrometer in the range 400–4000 cm^{-1}. High-resolution liquid secondary ion mass spectra (HR LSI MS) were measured on a VG ZabSpec mass spectrometer (conditions: positive ion mode, 2-nitrophenyl octyl ether or 3-nitrobenzyl alcohol matrix, CsI primary ion source).

Electrochemical measurements were performed with a computer-controlled multipurpose potentiostat μAutolab III (Eco Chemie, The Netherlands) at room temperature, using a standard Metrohm three-electrode cell with a platinum disc (Autolab RDE, 3 mm diameter) working electrode, a platinum sheet auxiliary electrode, and a saturated calomel reference electrode which was separated from the analysed solution by a salt-bridge (0.2 M Bu_4NPF_6 in CH_2Cl_2). The analysed compounds were dissolved in dichloromethane (Fluka absolute, declared water content ≤ 0.005%) to give a solution containing 5×10^{-4} M analyte and 0.2 M Bu_4NPF_6 (Fluka, purissimum for electrochemistry) as the supporting electrolyte. The solutions were deaerated with argon before the measurements and then kept under an argon blanket. The redox potentials are given relative to the standard ferrocene/ferrocenium reference.

Preparation of $[Ru_2(\mu\text{-}HCO_2)_2(CO)_4(FcPPh_2)_2]$ (**3**)

A suspension of (diphenylphosphino)ferrocene (0.296 g, 0.78 mmol) and **1** (0.152 g, 0.75 mmol Ru) in toluene (15 ml) was heated to reflux for 30 min, whereupon the solid reagents dissolved to give a clear yellow solution. The solution was cooled to room temperature and evaporated under reduced pressure. The solid residue was washed carefully with diethyl ether (5 ml) and petroleum ether (5× 5 ml), and dried at 100 °C for 1 h to afford **3**

as a bright yellow solid. Yield 0.390 g (91%). ^{1}H NMR ($CDCl_3$): 4.17 (s, 5 H, C_5H_5), 4.37 (br s, 2 H, CH of C_5H_4), 4.48 (br apparent t, 2 H, CH of C_5H_4), 7.33–7.61 (m, 10 H, PPh_2), 8.32 (s, 1 H, HCO_2). ^{13}C NMR ($CDCl_3$): 69.6 (s, C_5H_5), 71.3 (virtual t, J' = 3, CH of C_5H_4), 73.7 (virtual t, J' = 5, CH of C_5H_4), 76.3 (virtual t, J' = 18, C_{ipso} of C_5H_4), 127.7 (virtual t, J' = 5, CH_m of PPh_2), 129.4 (s, CH_p of PPh_2), 133.3 (virtual t, J' = 6, CH_o of PPh_2), 136.2 (virtual t, J' = 17, C_{ipso} of PPh_2), 176.1 (virtual t, J' = 8, HCO_2), 204.9 (virtual t, J' = 4, C≡O). ^{31}P{^{1}H} NMR ($CDCl_3$): +4.4 (s). IR (Nujol): ν(C≡O) 2029 (s), 1987 (s), 1954 (s); ν(C=O) 1600 (s), 1587 (s); 1303 (m), 1164 (m), 1108 (m), 1097 (m), 1031 (m), 823 (m, composite), 746 (m), 741 (m), 694 (m), 575 (m), 431–538 (m, composite). For $C_{50}H_{40}Fe_2O_8P_2Ru_2$ calculated: 52.47% C, 3.52% H; found: 52.14% C, 3.97% H. HR LSI MS: for $C_{50}H_{40}{}^{56}Fe_2O_8P_8{}^{102}Ru_2$ (M^+) calculated 1145.8984, found 1145.8973.

Preparation of $[Ru_2(\mu\text{-}CH_3CO_2)_2(CO)_4(FcPPh_2)_2]$ (**4**)

Complex **4** was prepared as described for **3**, starting with $FcPPh_2$ (0.296 g, 0.80 mmol) and **2** (0.162 g, 0.75 mmol Ru) in toluene (15 ml). Refluxing for 1 h and isolation as above gave **4** as a bright yellow-orange solid. Yield 0.412 g (94%). ^{1}H NMR ($CDCl_3$): 1.85 (s, 3 H, O_2CCH_3), 4.16 (s, 5 H, C_5H_5), 4.42 (m, 2 H, CH of C_5H_4), 4.48 (apparent t, J' = 1.8, 2 H, CH of C_5H_4), 7.31–7.61 (m, 10 H, PPh_2). ^{13}C NMR ($CDCl_3$): 23.5 (s, O_2CCH_3), 69.5 (s, C_5H_5), 71.2 (virtual t, J' = 3, CH of C_5H_4), 73.7 (virtual t, J' = 5, CH of C_5H_4), 76.4 (virtual t, J' = 18, C_{ipso} of C_5H_4), 127.5 (virtual t, J' = 5, CH_m of PPh_2), 129.2 (s, CH_p of PPh_2), 133.5 (virtual t, J' = 6, CH_o of PPh_2), 136.4 (virtual t, J' = 17, CH_{ipso} of PPh_2), 185.7 (virtual t, J' = 8, O_2CCH_3), 205.5 (virtual t, J' = 4, C≡O). ^{31}P{^{1}H} NMR ($CDCl_3$): +5.0 (s). IR (Nujol): ν(C≡O) 2018 (s), 1971 (s), 1943 (s); ν(C=O) 1576 (s); 1306 (m), 1163 (m), 1108 (m), 1095 (m), 1029 (m), 826 (m, composite), 752 (m), 744 (m), 698 (m), 584 (m), 433–541 (m, composite). For $C_{52}H_{44}Fe_2O_8P_2Ru_2$ calculated: 53.26% C, 3.78% H; found: 53.00% C, 3.57% H. HR LSI MS: for $C_{52}H_{44}{}^{56}Fe_2O_8P_2{}^{102}Ru_2$ (M^+) calculated 1173.9297, found 1173.9327.

Reaction of **2** with Hdpf

The reaction of **2** (0.75 mmol) with Hdpf (0.80 mmol) gave a bright orange-yellow powder, which was completely insoluble in common organic solvents, including the highly polar and/or coordinating ones (e.g., dimethyl sulfoxide, *N*,*N*-dimethylformamide, acetone, acetonitrile, chloroform, dichloromethane and diethyl ether). The IR spectrum (as a Nujol mull) of the product showed strong bands attributable to ν(C≡O) 2020, 1979 and 1946, and carboxylate ν(C=O) 1553 (cf. 1666 for solid Hdpf [6a]). Further IR bands: 1358 (s), 1195 (m), 1162 (m), 1095 (m), 1031 (m), 834 (br m), 806 (w), 788 (w), 742 (m), 694 (s), 490–534 (composite m).

X-ray Crystallography

Single crystals of **4** suitable for X-ray diffraction analysis were grown from hexane–dichlomethane by liquid-phase diffusion at 4 °C (selected specimen: orange prism, 0.25 × 0.25 × 0.47 mm^3). Full-set diffraction data ($\pm h \pm k \pm l$; $2\theta < 55°$) were collected with a Nonius KappaCCD diffractometer at 150(2) K (Oxford Cryosystem cooler) using graphite-monochromatized MoKα radiation (λ = 0.71073 Å). The data were corrected for absorption (μ(MoKα) = 1.354 mm^{-1}) using a Gaussian absorption correction based on indexed crystal shape as included in the diffractometer software. The range of the transmission coefficients

was 0.640–0.795. Crystallographic data: $C_{52}H_{44}Fe_2O_8P_2Ru_2$ (1172.65 g mol^{-1}), monoclinic, space group $P2_1/c$ (No. 14), a = 15.2470(2) Å, b = 16.5890(2) Å, c = 18.9688(2) Å; β = 100.4509(7)°, V = 4718.2(1) Å^3, Z = 4, D_{calc} = 1.651 g ml^{-1}.

The structure was solved by direct methods (SIR97 [14]) and refined by full matrix least-squares procedure based on F^2 (SHELXL97 [15]). All non-hydrogen atoms were refined with anisotropic displacement parameters. The hydrogen atoms were included in their calculated positions and refined as riding atoms. Refinement parameters were as follows: 82130 total, 10817 independent, and 9416 observed ($I > 2\sigma(I)$) diffractions; 595 parameters, R(observed data) = 2.63%, R(all data) = 3.38%, wR(all data) = 6.50%, largest peak and hole on the final difference electron density map: 1.05 and –0.68 e Å^{-3}. All post-refinement calculations were performed with a recent version of the PLATON program[16]. Numerical values are rounded with respect to their standard estimated deviations given with one decimal place.

CCDC 718096 contains the supplementary crystallographic data for this paper. These data can be obtained free of charge via www.ccdc.cam.ac.uk/conts/retrieving.html (or from the Cambridge Crystallographic Data Centre, 12, Union Road, Cambridge, CB2 1EZ, UK; fax: +44 1223 336033; or deposit@ccdc.cam.ac.uk).

This work is a part of the long-term research plan of Faculty of Science, Charles University, supported by the Ministry Education, Youth and Sports of the Czech Republic (project MSM 0021620857).

REFERENCES

1. Crooks G. R., Johnson B. F. G., Lewis J., Williams I. G., Gamlen G.: *J. Chem. Soc. A* **1969**, 2761.
2. a) Bianchi M., Matteoli U., Menchi G., Frediani P., Piacenti F.: *J. Organomet. Chem.* **1982**, *240*, 65; b) Matteoli U., Bianchi M., Menchi G., Frediani P., Piacenti F.: *J. Mol. Catal.* **1985**, *29*, 269; c) Matteoli U., Menchi G., Bianchi M., Piacenti F.: *J. Organomet. Chem.* **1986**, *299*, 233; d) Jenck J., Kalck P., Pinelli E., Siani M., Thorez A.: *J. Chem. Soc., Chem. Commun.* **1988**, 1428; e) Wolfender J. L., Neumann F., Süss-Fink G.: *J. Organomet. Chem.* **1990**, *389*, 351; f) Matteoli U., Menchi G., Bianchi M., Piacenti F.: *J. Mol. Catal.* **1991**, *64*, 257; g) Kalck P., Siani M., Jenck J., Peyrille B., Peres Y.: *J. Mol. Catal.* **1991**, *67*, 19; h) Rotem M., Shvo Y.: *J. Organomet. Chem.* **1993**, *448*, 189; i) Neveux M., Seiller B., Hagedorn F., Bruneau C., Dixneuf P. H.: *J. Organomet. Chem.* **1993**, *451*, 133; j) Darcel C., Bruneau C., Dixneuf P. H., Neef G.: *J. Chem. Soc., Chem. Commun.* **1994**, 333; k) Bruneau C., Kabouche Z., Neveux M., Seiller B., Dixneuf P. H.: *Inorg. Chim. Acta* **1994**, *222*, 155; l) Matteoli U., Menchi G., Bianchi M., Piacenti F., Ianelli S., Nardelli M.: *J. Organomet. Chem.* **1994**, *498*, 177; m) Seiller B., Bruneau C., Dixneuf P. H.: *Synlett* **1995**, 707; n) Seiller B., Bruneau C., Dixneuf P. H.: *Tetrahedron* **1997**, *51*, 13089; o) Lavastre O., Bebin P., Marchaland O., Dixneuf P. H.: *J. Mol. Catal. A: Chem.* **1996**, 108, 29; p) Darcel C., Bruneau C., Dixneuf P. H., Roberts S. M.: *Tetrahedron* **1997**, *53*, 9241; q) Bruneau C., Neveux-Duflos M., Dixneuf P. H.: *Green Chem.* **1999**, *1*, 183; r) Picquet M., Bruneau C., Dixneuf P. H.: *Tetrahedron* **1999**, *55*, 3937; s) Emme I., Bruneau C., De Meijere A., Dixneuf P. H.: *Synlett* **2000**, 1315; t) Salvini A., Frediani P., Piacenti F.: *J. Mol. Catal. A: Chem.* **2000**, *159*, 185; u) Le Gendre P., Comte V., Michelot A., Moise C.: *Inorg. Chim. Acta* **2003**, *350*, 289; v) Salvi L., Salvini A., Micoli F., Bianchini C., Oberhauser W.:

J. Organomet. Chem. **2007**, *692*, 1442; w) Micoli F., Oberhauser W., Salvini A., Bianchini C.: *J. Organomet. Chem.* **2007**, *692*, 2334.

3. a) Deschenaux R., Donnio B., Rheinwald G., Stauffer F., Süss-Fink G., Velker J.: *J. Chem. Soc., Dalton Trans.* **1997**, 4351; b) Frein S., Auzias M., Sondenecker A., Vieiller-Petit L., Guintchin B., Maringa N., Süss-Fink G., Barberá J., Deschenaux R.: *Chem. Mater.* **2008**, *20*, 1340.
4. a) Süss-Fink G., Wolfender J. L., Neumann F., Stoeckli-Evans H.: *Angew. Chem.* **1990**, *102*, 447; b) Shiu K.-B., Lee C.-H., Lee G.-H., Wang Y.: *Organometallics* **2002**, *21*, 4013; c) Shiu K.-B., Lee H.-C., Lee G.-H., Ko B.-T., Wang Y., Lin C.-C.: *Angew. Chem. Int. Ed.* **2003**, *42*, 2999.
5. a) Auzias M., Therrien B., Labat G., Stoeckli-Evans H., Süss-Fink G.: *Inorg. Chim. Acta* **2006**, *359*, 1012; b) Auzias M., Süss-Fink G., Štěpnička P., Ludvík J.: *Inorg. Chim. Acta* **2007**, *360*, 2023.
6. a) Podlaha J., Štěpnička P., Císařová I., Ludvík J.: *Organometallics* **1996**, *15*, 543; b) Štěpnička P.: *Eur. J. Inorg. Chem.* **2005**, 3787.
7. a) Pregosin P. S., Kunz R. W. in: *NMR Basic Principles and Progress* (P. Diehl, E. Fluck and R. Kosfeld, Eds), Vol. 16, Chap. E, p. 65 ff., and references therein; b) Hersch W. H.: *J. Chem. Educ.* **1997**, *74*, 1485.
8. Similar features have been observed in the spectra of *trans*-$[PdCl_2(Ph_2PFcX\text{-}\kappa P)_2]$ (X = CO_2H, PO_3Et_2, $CH{=}CH_2$) and *trans*-$[W(CO)_4(Ph_2PFcCH{=}CH_2\text{-}\kappa P)_2]$: a) Štěpnička P., Podlaha J., Gyepes R., Polášek M.: *J. Organomet. Chem.* **1998**, *552*, 293; b) Štěpnička P., Císařová I., Gyepes R.: *Eur. J. Inorg. Chem.* **2006**, 926; c) Štěpnička P., Císařová I.: *Collect. Czech. Chem. Commun.* **2006**, *71*, 215; d) Štěpnička P.: *J. Organomet. Chem.* **2008**, *693*, 297.
9. A search in the Cambridge Structural Database, version 5.30 of November 2008 resulted in 20 crystal structures containing 24 crystallographically independent $[Ru_2(\mu\text{-}CO_2)_2(CO)_4L_2]$ moieties, where L is any phosphine, showing the Ru–Ru distances in the range 2.716–2.760 Å. The deposition codes are as follows: ACBRUA10, BURPRU, KEHZIH, KEHZON, MUBTAE, MUBTEI, NIMZUE, QATMII, SEDKOB, UKADOZ, UKADUF, VISMAM, VISMEQ, WATFAY, WATFEC, WATFIG, YEDCOA, ZERROD, ZERRUJ, ZERSAQ.
10. Shiu K.-B., Peng S.-M., Cheng M.-C.: *J. Organomet. Chem.* **1993**, *452*, 143.
11. The atoms forming both planes are coplanar within less than 0.07 Å.
12. DDQ: $E^{\circ\prime}$ = 0.13 V in MeCN. For a reference, see: Connelly N. G., Geiger W. E.: *Chem. Rev.* **1996**, *96*, 877.
13. a) Sollot G. P., Mertwoy H. E., Portnoy S., Snead J. L.: *J. Org. Chem.* **1963**, *28*, 1090; b) Kotz J. C., Nivert C. L.: *J. Organomet. Chem.* **1973**, *52*, 387.
14. Altomare A., Burla M. C., Camalli M., Cascarano G. L., Giacovazzo C., Guagliardi A., Moliterni A. G. G., Polidori G., Spagna R.: *J. Appl. Crystallogr.* **1999**, *32*, 115.
15. Sheldrick G. M: *SHELXL97. Program for Crystal Structure Refinement from Diffraction Data*. University of Göttingen, Göttingen 1997.
16. a) Spek A. L.: *PLATON – A Multipurpose Crystallographic Tool*. Utrecht University, Utrecht 2003 and updates; b) Spek A. L.: *J. Appl. Crystallogr.* **2003**, *36*, 7.